HiSST: International Conference on
High-Speed Vehicle Science Technology
26–29 November 2018, Moscow, Russia

ADVANCE: A space vehicle analysis and design tool

Ph. Reynier[1], J. Van den Eynde[2] and J. Steelant[2]

Abstract

Software generally used for the post processing of CFD calculations are limited to generic flow variables such as pressure, density, velocity, Mach number... In the perspective of the in-depth analysis of CFD results some other parameters such as Reynolds number, shock-layer thickness are of interest. The purpose of this work has for objective to cover this gap.

This contribution focuses on the development of a software dedicated to the post-processing of computational fluid dynamics results, with as ultimate objective to be a tool dedicated to the design analysis of spacecraft. At first, the parameters of interest for describing the boundary layer main characteristics (thickness, occurrence of transition) have been selected from the literature. In parallel an extensive survey of similar tools have been carried out for selecting the best approach for the software to be developed.

Here, the first results obtained with this tool on two configurations are presented. The first one is a slender body, while the other is a Mars entry probe.

Keywords : *Post-processing, design, optimization, transition to turbulence, hypersonics*

Nomenclature

[1] *Ingénierie et Systèmes Avancés, Mérignac, France , Philippe.Reynier@isa-space.eu*
[2] *ESA-ESTEC, Aerothermodynamics and Propulsion Analysis Section TEC-MPA, P.O. Box 299, Noordwijk, Netherlands, Jeroen.van.den.Eynde@esa.int, Johan.Steelant@esa.int.*

b	Bluntness
C_f	Friction coefficient
h	Enthalpy
M	Mach number (free stream)
Nu	Nusselt number
P	Pressure
Pr	Prandtl number
Q	Heating rate
R	Radius (cm)
Re	Reynolds number
S	van Driest compressibility factor
St	Stanton number
T	Temperature
U, V, W	Velocity components in x, y, z directions
x, y, z	Cartesian coordinates
δ	Boundary layer thickness
δ_1	Displacement thickness
δ_2	Momentum thickness
δ_T	Thermal boundary layer thickness
δ_3	Energy thickness
μ	Dynamic viscosity
ν	Kinematic viscosity
ρ	Density
τ	Shear stress

Subscripts

aw	Adiabatic wall
e	Boundary-layer edge
f	Friction
k	roughness
t	Transition
w	wall
θ	Momentum thickness
∞	Free-stream
$*$	Reference

Acronyms

BL	Boundary Layer
BLT	Boundary Layer Transition
CFD	Computational Fluid Dynamics
TH	THermal boundary layer
TPS	Thermal Protection System

1. Introduction

Various aerothermodynamics phenomena have a strong impact on space-vehicle performances and their endurance towards the related harsh environment characterizing an atmospheric entry. These phenomena might either be induced by the intrinsic nature of the flow itself such as instabilities, transition, separations… or due to specific structural implementations of the aeroshell that can involve steps, gaps, irregularities, protuberances etc. Any of these effects might induce higher heat loads and/or increase aerodynamic drag, resulting in increasing the mass of the Thermal Protection System (TPS), the fuel consumption and/or reducing the cross range.

However, when carefully mastering these effects [1], a substantial reduction of the TPS mass (up to 15%-20% depending on vehicle characteristics and mission profile) or a 10% to 15% increase in cross range can be achieved compared to the usual baseline approach based on the assumption of a fully turbulent flow.

High-fidelity engineering simulation tools alone cannot assess the occurrence and the location of these critical phenomena. One actually needs to rely on empirical correlations [2] based upon local flow conditions and other parameters such as momentum thicknesses, Reynolds number, shock-layer thickness…

The objective of the present activity is to develop a software for analysing CFD numerical simulations, using the existing correlations for the assessment of the transition to turbulence, and more particularly to identify whether and where these critical flow phenomena occur. An example of such evaluation is shown in Fig 1. The objective is to help the design optimization and increase the vehicle performances as well as the provision of acceptable tolerances for steps and gaps near structural interfaces.

The main objective of this study is to demonstrate a proof of concept for such a design tool. Some of the parameters can be difficult to define around geometrical singularities such as stagnation points, sharp edges, corners… Therefore, the goal is to generate a first version of the software and to test it

around dedicated shapes. This will provide an assessment of its reliability for post processing and further extension of its capabilities.

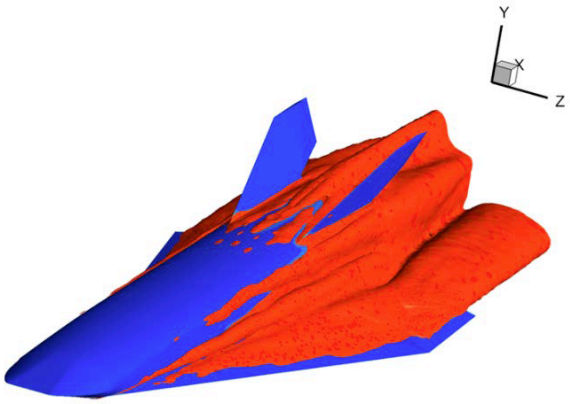

Fig 1: Transition flow assessment around a slender body [Erreur ! Signet non défini.]

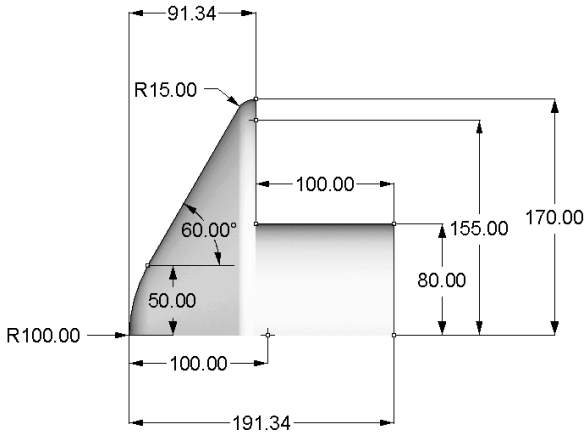

Figure 2: MSRO configuration [3]

2. Boundary Layer Characterization

2.1. Selected configurations

Two configurations have been selected for the study. The first one is the aeroshell of the Mars Sample Return Orbiter [3] shown in Figure 2. This corresponds to the Test Case 3 studied in the frame of the Radiation Working Group monitored by ESA. The second test case for the current study is a slender EFTV glider vehicle studied in [2] shown in Figure 3.

2.2. Boundary layer

For the purpose of post-analysis CFD, the following list of parameters has been identified for describing the boundary-layer:

- Displacement, momentum and energy thicknesses;
- Shape factor;
- Friction velocity;
- Pressure gradient;
- Separation points and inflexion of velocity profile;
- Velocity and thermal boundary-layer thicknesses;
- Edge values: temperature, pressure, velocity, density, Mach number;
- Local and reference Reynolds number.

The purpose of the software is to help the characterization of boundary-layer and aeroheating. Related to these two points the transition to turbulence is also of interest.

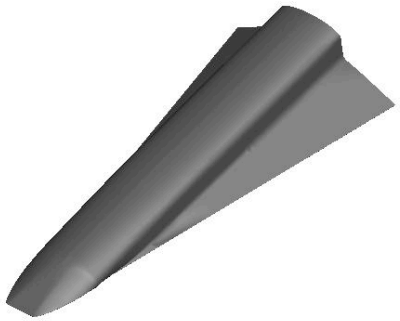

Figure 3: Slender vehicle configuration

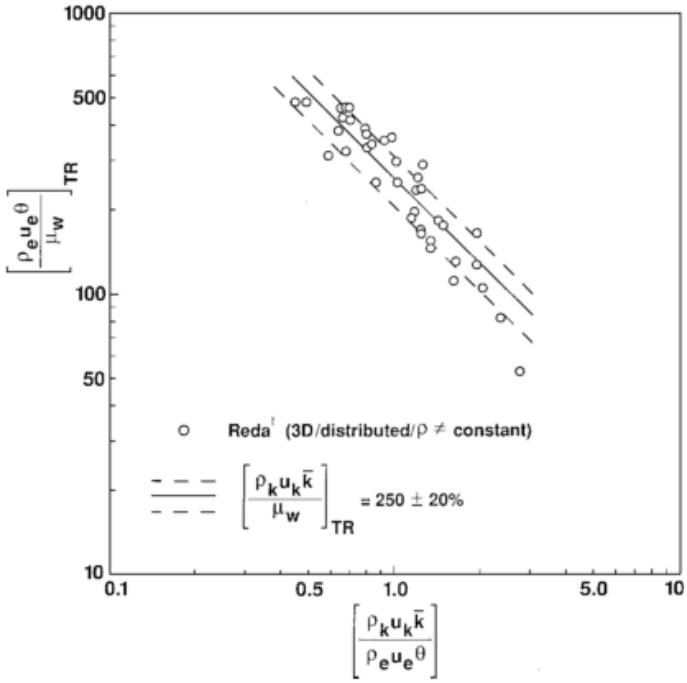

Figure 4: Nosetip transition data from ballistic-range tests [4]

For the purpose of post-analysis CFD, the most interesting point is to have a deep evaluation of the boundary-layer and related parameters. The following ones have been identified:

- Boundary-layer thickness, δ: defined as the layer where the velocity is less than 0.99 than the free-stream velocity (a user defined option will be also considered). If an Euler solution is available, the wall values of velocity, density, enthalpy, pressure and enthalpy will be used as free-stream values.
- Boundary-layer displacement thickness, δ_1, defined as,

$$\delta_1 = \int_0^{\delta} \left(1 - \frac{\rho u}{\rho_e u_e}\right) dy \tag{1}$$

- Boundary-layer momentum thickness, θ or δ_2, defined as,

$$\delta_2 = \int_0^{\delta} \frac{\rho u}{\rho_e u_e} \left(1 - \frac{u}{u_e}\right) dy \tag{2}$$

- Thermal boundary-layer thickness δ_T, defined as the layer where the velocity is less than 0.99 than the free-stream velocity (an user defined option will be also considered);
- Energy thickness, δ_3, defined as,

$$\delta_3 = \int_0^{\delta} \frac{\rho u}{\rho_e u_e} \left(\frac{h_t}{h_{t,e}} - 1\right) dy \quad \text{with} \quad h_t = h + \frac{u^2}{2} \tag{3}$$

- Local Reynolds number, Re;

$$Re_x = \frac{(\rho U)_e x}{\mu_e} \quad (4)$$

- Momentum thickness Reynolds number,

$$Re_\theta = \frac{(\rho U)_e \theta}{\mu_e} \quad (5)$$

- Roughness height Reynolds number [4] (see Figure 4),

$$Re_{kk} = \frac{(\rho U)_k k}{\mu_w} \quad \text{and} \quad Re_{ke} = \frac{(\rho U)_e k}{\mu_w} \quad (6)$$

- Edge values: temperature, T_e, pressure, P_e, density, ρ_e, and viscosity, μ_e.

Where k is the local roughness, height; the subscripts e, k and w denote respectively the variables taken at the boundary-layer edge, at the roughness height and at the wall.

2.3. Transition to turbulence

The location of transition to turbulence onset along al flight trajectory is an important parameter when designing an aerospace vehicle. This phenomenon has a strong impact on vehicle performances and TPS design [5]. A careful monitoring of the transition altitude and the transition location [6] over the vehicle surface can allow a substantial reduction of the TPS weight (up to 15%-20% depending on vehicle characteristics and mission profile) when comparing to the classical conservative approach where the design is based on the assumption of turbulent heating. An improving handling of potential transition location would have a definite positive impact for expandable and reusable launchers as well as for re-entry and entry vehicles with increased payloads and/or capabilities (see **Erreur ! Source du renvoi introuvable.**). Also the gliding performance or the aerodynamic efficiency can considerably increase (up to 10 to 15% [7]) and predicted by identifying where and when critical phenomena occur. This could then also guide the designer for further geometry improvements for enhancing the vehicle (shuttles, slender body, scramjets) performances or reducing weight.

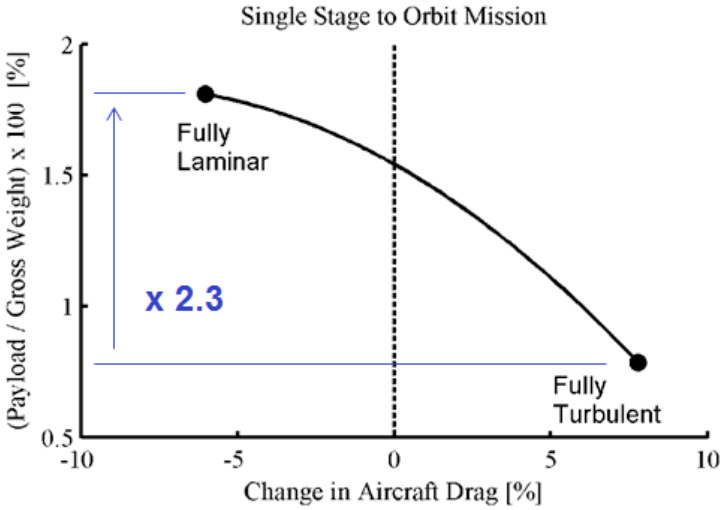

Figure 5: Boundary layer effect on drag and payload [8]

However, the prediction of transition to turbulence location along a trajectory of over a vehicle surface is a difficult issue. Some empirical or semi-empirical criteria are available but they are generally not handled automatically by available post processing software. Tools generally used for the post processing of CFD calculations are limited to generic flow variables such as pressure, density, velocity, Mach number... In the perspective of the in-depth analysis of CFD results (or also experimental datasets) some other parameters such as Reynolds number, shock-layer thickness, thermal shock-layer thickness, transition criteria are of interest. These kinds of parameters can be key points for the analysis of numerical simulations. Concerning space applications, they are of interest for the aerothermal design of space vehicles such as launchers, planetary entry probes, and slender vehicles including scramjets.

The purpose of this activity has as objective to pave the way to cover this gap. As a consequence the purpose of the activity is to generate a first version of the software and to test it around dedicated shapes. Different criteria have been used in [**Erreur ! Signet non défini.**] for estimating the

occurrence of transition over a slender vehicle. Some of them have been selected for this proof of concept, they are retained for the study, and detailed hereafter.

The criteria retained are those proposed by Simeonides and Berry (reported in [**Erreur ! Signet non défini.**]). Those of Simeonides [9] are based on the estimate of the transition location onset and transition zone length, and depend on the leading edge bluntness, as follows:

Weak bluntness for,

$$Re_b < 70\, M_\infty^{1.7} \qquad Re_t = 0.9\, \frac{Re_\infty}{M_\infty} \tag{7}$$

Where M_∞ is the free-stream Mach number. Re_∞ is calculated for a characteristic length of 1 m. Re_b is the bluntness Reynolds number based on the free-stream conditions and the leading edge thickness.

Moderate bluntness for,

$$Re_b < 1000\, M_\infty^2 \qquad Re_t = 70000\, M_\infty^{0.08}\, Re_b^{0.46} \tag{8}$$

Strong bluntness for,

$$Re_b > 1000\, M_\infty^2 \qquad Re_t = 6\, 10^6\, M_\infty^{1.38} Re_b^{-0.19} \tag{9}$$

For a cone we have,

$$Re_t = 5\, 10^5\, M_\infty^{0.8}\, Re_b^{0.1} \tag{10}$$

The transition length is given by the following relation valid for a flat plate,

$$Re_{\Delta x} = (60 + 4.86\, M_\infty^{1.92})\, Re_t^{2/3} \tag{11}$$

Berry has proposed a criterion used for the NASP and X43 projects. It is based on the Reynolds momentum thickness and the boundary layer edge Mach number as,

$$Re_\theta \geq 300\, M_e \tag{12}$$

These criteria are based on a certain degree of empiricism; here they have been selected in order to have an easy integration in the final tool.

2.4. Heating estimate

The local heat transfer can be expressed either the Nusselt and/or Stanton numbers [10]. They are defined as,

$$Nu = \frac{x\, q_w}{k_e\, (T_{aw} - T_w)} \tag{13}$$

$$St = \frac{q_w}{\rho_e U_e\, (h_{aw} - h_w)} \tag{14}$$

Where aw denotes the adiabatic wall value, and x the distance to the stagnation point The Nusselt number depends on the thermal conductivity, this quantity is not always directly available from CFD computational results. As a consequence, it is generally more convenient to select the Stanton number. This last can be estimated using the Reynolds analogy [11], using the following correlations:

$$St = \frac{\tau_w}{\rho_e\, U_e^2} \tag{15}$$

The relation is valid for laminar conditions and without wall injection. The quantity, τ_w, is the wall shearing defined as,

$$\tau_w = \left(\mu \frac{\partial U}{\partial y}\right)_w \tag{16}$$

Steelant & al [**Erreur ! Signet non défini.**] have used the following correlations for computing the Stanton number (based on Reynolds analogy). For laminar flows we have,

$$St = \frac{Cf}{2\, Pr^{2/3}} = \frac{1}{2\, Pr^{2/3}}\, \frac{0{,}664}{Re_{xe}^{1/2}} \sqrt{\frac{\mu^* T_e}{\mu_e T^*}} \tag{17}$$

where T* is the reference temperature, defined in [24] as,

$$\frac{T^*}{T_e} = 1 + 0.54\left(\frac{T_w}{T_e} - 1\right) + 0.16\, r\, \frac{\gamma-1}{2} M_e^2 \tag{18}$$

For turbulent flows:

$$St = \frac{Cf}{2\, Pr^{2/3}} = \frac{1}{2\, Pr^{2/3}} \frac{0{,}455}{S^2 \ln^2\left(\frac{0{,}06}{s} Re_{xe} \frac{\mu_e}{\mu_w}\sqrt{T_e/T_w}\right)} \tag{19}$$

where S^2 is the Van Driest compressibility factor. These two correlations compare well with experimental data, as a consequence they will be selected for the current study.

An alternative is to use the correlations for the Stanton number, available in [24] and valid for a flat plate. They are based on a power profile for the velocity estimating the Stanton number via the Reynolds analogy,

$$St = k\, f\, /\, Re_x^{s0} \tag{20}$$

Where k and s0 are, for laminar flows, equal to 0.823 and 1/2 respectively, and, for turbulent flows, to 0.0274 and 1/6 respectively. The function *f* is defined by the relations (29) and (30).

Friction coefficient will be estimated as follows for laminar flows,

$$C_f = \frac{0{,}664}{Re_{xe}^{1/2}} \sqrt{\frac{\mu^* T_e}{\mu_e T^*}} \tag{21}$$

For turbulent flows,

$$C_f = \frac{0{,}455}{S^2 \ln^2\left(\frac{0{,}06}{s} Re_{xe} \frac{\mu_e}{\mu_w}\sqrt{T_e/T_w}\right)} \tag{22}$$

Like for the Stanton number,, an alternative is also to use the correlations from [24]:

$$Cf = k\, f\, /\, Re_x^{s0} \tag{23}$$

Where k and s0 are, for laminar flows, equal to 0.664 and 1/2 respectively (correlation (21) is recovered), and, for turbulent flows, to 0.0368 and 1/6 respectively. The function is f defined by the relations (29) and (30).

Thermal boundary layer thickness can be estimated using temperature or enthalpy,

$$T^+ = |T - T_w|/\lfloor T_\infty - T_w \rfloor \tag{24}$$

$$h^+ = |h - h_w|/\lfloor h_\infty - h_w \rfloor \tag{25}$$

Like for the velocity, a cut-off value of 0.99 is retained with the possibility to have a user-provided value.

For axisymmetric solutions, the correlations need to be scaled according to:

$$\frac{\delta_{2,cone}}{\delta_{2,plate}} = \left(\frac{1}{m_0+2}\right)^{\frac{1}{m_0+1}} \tag{26}$$

$$\frac{C_{f,cone}}{C_{f,plate}} = (m_0+1)^{\frac{1}{m_0+1}} \tag{27}$$

where the parameter value m_0 depends on state of the boundary layer, with laminar and turbulent values of 1 and 1/5 respectively. The definition and correlation of H (see Eq. (34)) remains unchanged.

2.5. Summary

To summarize, the following parameters of interest have been identified:

- Local Reynolds number, Re;
- Flow Mach and Reynolds numbers;
- Stagnation enthalpy;
- Friction coefficient;
- Momentum thickness Reynolds number;

- Roughness height values: Reynolds number, velocity, density, viscosity;
- Thermal and velocity boundary-layer thickness;
- Displacement, momentum and energy thicknesses;
- Local Stanton number;
- Wall shearing;
- Friction velocity;
- Pressure gradient;
- Separation points and inflexion of velocity profile;
- Shape factor;
- Edge values: temperature, velocity, viscosity, enthalpy, and Mach number;
- Wall values: temperature, viscosity, and enthalpy.

3. Tool development

3.1. Existing software survey

A review of CFD and/or similar tools has been undertaken in the following directions:

- CFD open source tools;
- Available NASA tools [12];
- Software from LLNL [13];
- INRIA tools [14];
- SCILAB [15];
- CASSIOPEE from ONERA [16].

Two CFD open source package have been surveyed: OpenFoam [17] and SU^2 from Stanford University [18]. Unfortunately, these two software does not present features or interest for the current project. However, tools can be developed for such purposes, as highlighted in [19], where a Python script is used for mesh refinement of CFD calculations carried out with OpenFoam.

The survey of NASA open source tools, did not highlight the existence of a similar software that the one to be developed within the current effort. The tools with for objective to manipulate datasets can be Excel macro, or written in C, Matlab, or Python. A quick survey, has shown that the most relevant, such as AbVerify (to manipulate ABAQUS datasets), are written in Python.

Among the software from LLNL, Visit is a visualisation tool that can be downloaded. This graphic software can be considered to be an equivalent of Tecplot, even if it does not provide the same level of available options.

INRIA has developed a large number of open source software [14], certain dedicated to computational physics. However, none of them could cover the objective of the current effort. Among all these open source tools Scikit Learn [20], written in Python, is dedicated to data analysis (classification, clustering, regression) but more focused on statistical applications and any field requiring robust machine-learning solutions.

SCILAB [15] is an open source software initially developed by INRIA and dedicated to numerical computations. It provides an environment for the development of scientific and engineering applications. This software uses different languages such as C, C^{++}, Java… However, the use of SCILAB would not ease the development of ADVANCE since the usual boundary layer correlations would have to be incorporated in the tool. Additionally, there is no compatibility between with Tecplot, SCILAB using its own format for input and output files.

CASSIOPEE [16] is an open source tool developed by ONERA for pre- and post-processing purposes. It is built in Python and has two modules, one for pre-processing of meshes the other for the post-processing of CFD results. The last one allows features such as the extraction of isosurfaces, and the interpolation of CFD fields. The compatibility of the tool to the Tecplot format is not documented.

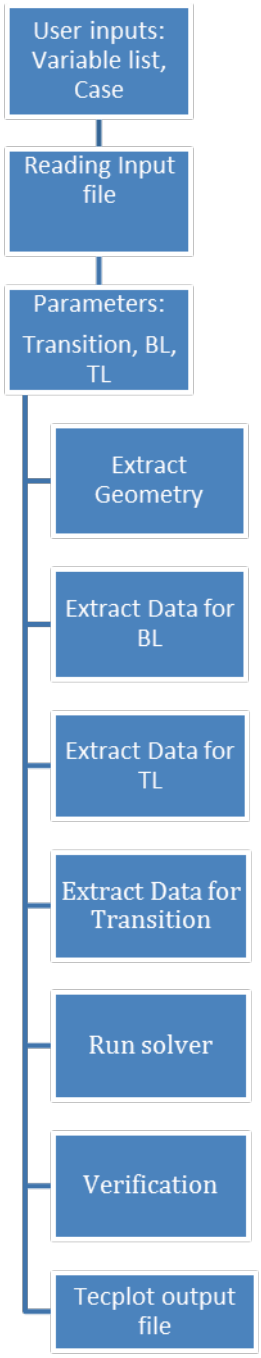

Figure 6: Software architecture

3.2. Overall strategy and Architecture

The main outcome of the review is the absence of similar software among the reviewed open source tools. However, the survey has also provided other outcomes. The main issue is that these tool are not dedicated to extract boundary layer parameters from CFD results. This confirms the need to develop a tool dedicated to the current objective of this project.

When looking at the languages used for the available tools, some are utilizing different languages some are based on Java, C, C^{++}, Python…. This applies particularly to the CFD post-processing tool developed by ONERA, CASSIOPEE, which is built in Python, C^{++} and Fortran 90. However, in this last case all the user interface is made in Python. This shows the relevance of such approach for the tool to be developed. Here, the objective is to have an easy access to the tool by the users and a common data representation. For such objectives, Python presents some assets: it is fast to start with,

generally easy to use, and well spread in the scientific community. Generally, different Python libraries are present in the current Linux distributions.

The final tool will have to be compatible with Tecplot: this means the input files have to be readable by Tecplot (with the option Tecplot Data Loader when selecting import format in Tecplot), and the same will apply to the outputs. It will be built with Python with, if necessary, modules developed in Fortran 90.

Different empirical criteria can be used to estimate parameters such as transition, boundary layer characteristics, and surface heating; therefore a GUI interface shall be implemented to give such choice to the user.

The tool architecture will be articulated as resumed in Figure 6. The different parts are detailed hereafter:

- User input: 2D, axisymmetric, or 3D configuration, choice of the case (i.e. boundary layer, thermal layer, or transition), variable list and mesh cell numbers (and blocks) in the input file. Other inputs are environment (air or CO_2), perfect gas constant value (default can be 1.4 for air and 1.3 for CO_2), option with user provided gas constant will be also considered. S for Sutherlands' law (default values can be 110 K for air and 254 K for CO_2).
- Reading file: Reading of input file using Tecplot Data Loader in Select Import Format option in Tecplot.
- Parameters: Definition of relevant parameters to be extracted or computed depending on the case (i.e. boundary layer, thermal layer, or transition) selected.
- Extraction of body geometry from mesh (alternative is to have a separate surface file as input).
- Extract parameters: extract from data the values of various variables at different heights: edge, wall, infinity, and prescribed height if applicable. For that purpose, a normal to the wall will be defined, the values will be computed by interpolation from the neighbouring points. To extract a normal from a quadrilateral, it is proposed to use the cross-product of the diagonals of the control volume.
- Run solver: Calculation of necessary data depending on the selected case (BL, TL, or transition (BLT)). In some correlations quantities are function of x as they were developed for a flat plate. In 2D, the curvilinear coordinate can be introduced and uses as first approximation. In 3D the curvilinear coordinate can also be introduced but the streamline length is a far better choice but a more complex one, since it requires assessing the corresponding stagnation point. This method will be attempted in the tool and is the approach preferred by ESA.
- Verification: Data verification (see following section), in order to give the user an estimate of the calculation reliability. Additionally, computed values of differences between calculated and theoretical data pondered by the theoretical values will be provided as output.
- Tecplot output compatible file: Writing outputs readable in Tecplot.

3.3. Verification

The last part of this technical note focuses on the verification of the results provided by the tool. For this purpose, the outputs of the software have to be compared with experimental or theoretical data. Experimental data are not always available; as a consequence, the most convenient way is to use theoretical or empirical correlations when available.

The most critical point is a good assessment of the boundary layer, since all other correlations are depending on it. Then, the effort has been focused on this point. Different correlations are available in the literature [21, 22, 23]. However, correlations provided by ESA [**Erreur ! Signet non défini.**,24] have been retained for the current effort. They are valid for laminar and turbulent flows.

The correlations provide the displacement, momentum, and boundary layer thicknesses. They have been established for a flow over a flat plate with the assumption of a constant specific heat capacity.

	r	s_0	k_1	H_i	α	β
Laminar	0.85 or $Pr^{1/2}$	1/2	0.664	2.591	0.667	2.9
Turbulent	0.9 or $Pr^{1/3}$	1/6	0.0221	1.4	0.4	1.222

Table 1: Values of the different constants for laminar and turbulent conditions (r= Pr1/2

The momentum thickness is given as,

$$\delta_2 = k_1 f x / Re_x^{s_0} \tag{28}$$

Where k_1 and s_0 are given in Table 1 for laminar and turbulent conditions; whereas f is given as for laminar flows as,

$$f = \left(\frac{\rho^* \mu^*}{\rho_e \mu_e}\right)^{1/2} \tag{29}$$

and for turbulent flows as,

$$f = \left(\frac{\rho^*}{\rho_e}\right)^{5/6} \left(\frac{\mu^*}{\mu_e}\right)^{1/6} \tag{30}$$

where the viscosity dependency is given by the Sutherland's law:

$$\frac{\mu^*}{\mu_e} = \left(\frac{T^*}{T_e}\right)^{1/2} \frac{1+S/T_e}{1+S/T^*} \tag{31}$$

with S = 110.4 K for air and 254 K for CO_2.

$$\frac{\rho^*}{\rho_e} = \frac{T_e}{T^*} \tag{32}$$

The reference temperature T^* is given as,

$$\frac{T^*}{T_e} = 1 + 0.54\left(\frac{T_w}{T_e} - 1\right) + 0.16\, r\, \frac{\gamma-1}{2} M_e^2 \tag{33}$$

The values of r are reported in Table 1.

The ratio H between the displacement thickness and the momentum thickness, is,

$$\frac{\delta_1}{\delta_2} = H = H_i + \alpha M_e^2 + \beta \frac{T_w - T_f}{T_e} \tag{34}$$

The values for H_i, α, and β, are listed in Table 1.

Where the recovery, adiabatic wall or friction temperature $T_r = T_{aw} = T_f$ is given as,

$$\frac{T_f}{T_e} = 1 + r\, \frac{\gamma-1}{2} M_e^2 \tag{35}$$

The ratio between the boundary layer thickness and the displacement thickness for a laminar flow [24], is,

$$\frac{\delta}{\delta_1} = 1 + \frac{5}{2} \frac{2.591}{H} \tag{36}$$

For a turbulent flow [24],

$$\frac{\delta_1}{\delta} = 1 - n\, I_n \tag{37}$$

with I_n equal to,

$$I_n = \int_0^1 \frac{W^n}{\frac{T_w}{T_e} + \left(\frac{T_f - T_w}{T_e}\right) W - \left(\frac{T_f}{T_e} - 1\right) W^2} dW \tag{38}$$

With n equal to 5 and $W=u/u_e$.

These correlations will be plotted in a Tecplot file output in the form of a non-dimensional difference. This will give the user a comparison between the computed and theoretical values that will be also

plotted in true dimensions.

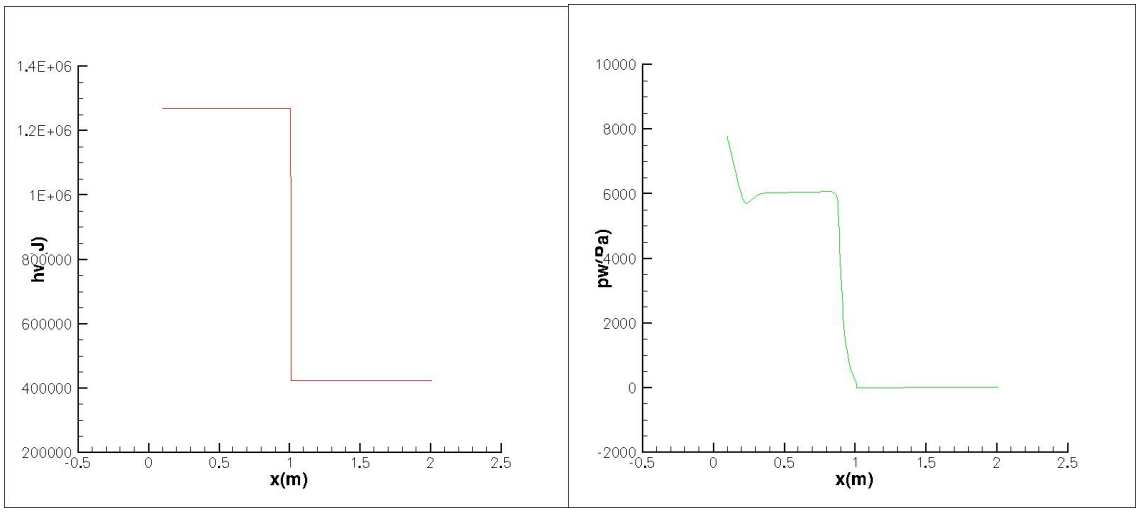

Figure 7: Wall enthalpy (left) and pressure (right) for a Mars probe

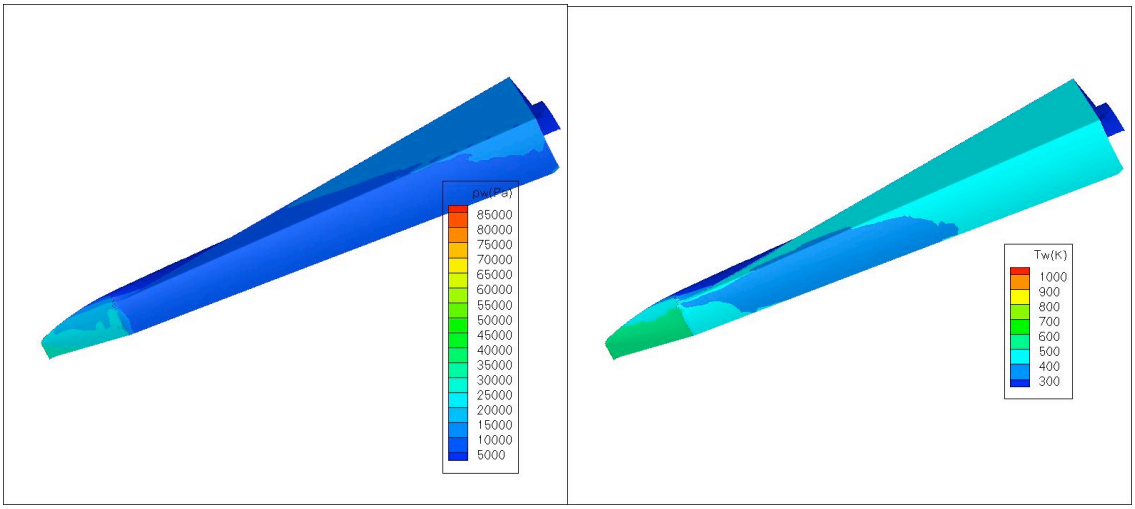

Figure 8: Wall pressure (left) and temperature (right) for a slender body

4. Preliminary results

The development of the tool has been undertaken and first results obtained for both configurations selected for the study. The first task has been to recover the wall parameters: density, dynamic viscosity, enthalpy, temperature, and pressure. This has been achieved and some of them (pressure, enthalpy, and temperature) are shown in Fig. 7 and 8 for the Mars probe and the slender body respectively.

Then, first calculations have been performed to estimate the Reθ along the surface. Results obtained for the Mars entry probe are shown in Fig. 9. They highlight the difficulty for estimate this quantity near sharp edges and corners.

In the final papers the results obtained for both configurations will be analysed in order to estimate the validity of the tool developed and its usefulness for designing future spacecraft.

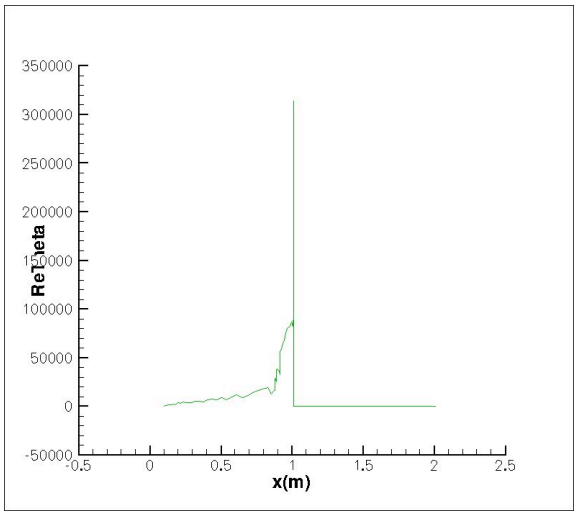

Figure 9: Distribution of Reθ along the wall of a Mars entry probe

References

[1] Hollis, B. R., Blunt body entry vehicle aerothermodynamics: transition and turbulence on the CEV and MSL configurations, AIAA Paper 2010-4984, 40th AIAA Fluid Dynamics Conference, Chicago, 28 Jun.-1 July 2010

[2] Steelant, J., Passaro, A., Fernandez-Villace, V., Gubanov, A. A., Ivanyushkin, D. S., Shvalev, Y. G., Voevodenko, N. V., Marini, M., and Di Benedetto, S., Boundary layer transition assessment on a slender high-speed vehicle, AIAA Paper 2017-2133, 21st International Space Planes and Hypersonic Technologies Conference, Xiamen, China, 6-9 March 2017.

[3] Omaly, P. and Druguet, M.-C., Workshop 2012 'Radiation of High Temperature Gas', TC3 : Update of the axially symmetric testcase for high temperature gas radiation prediction in Mars atmosphere entry, DCT/TV/PR-2012, Draft, CNES, 25 June 2012.

[4] Reda, D. C., Review and synthesis of roughness-dominated transition correlations for re-entry applications, Journal of Spacecraft and Rockets, Vol. 39(2), pp. 161-167, March-April 2002.

[5] Reshotko, E., Transition issues for atmospheric entry, Journal of Spacecraft and Rockets, Vol. 42(2), pp. 161-164, March-April 2008.

[6] Hollis, B. R., Blunt body entry vehicle aerothermodynamics: transition and turbulence on the CEV and MSL configurations, AIAA Paper 2010-4984, 40th AIAA Fluid Dynamics Conference, Chicago, 28 Jun.-1 July 2010

[7] Ponnappan, R., Turbulence and transition, Air Force Research Laboratory, Spring Review 2014, 3 March 2014.

[8] Whitehead, A., NASP aerodynamics, AIAA Paper 89-5013, 1st Aerospace Plane Conference, Dayton, Ohio, 20-21 July 1989.

[9] Simeonides, G. A., Laminar-turbulent transition correlations in supersonic/hypersonic flat plate flow, 24th International Congress or Aeronautical Sciences ,Yokohama, 29 Aug. – 3 Sept. 2004.

[10] Anderson, J. D., Hypersonics and High Temperature Gas Dynamics, McGraw-Hill Editions, New-York, 1989.

[11] Duffa, G., Ablative Thermal Protection Systems Modeling, AIAA Educational Series, 2013.

[12] NASA's Open Source Software, https://code.nasa.gov

[13] https://wci.llnl.gov/simulation/computer-codes

[14] https://www.icommunity.fr/patrimoine-technologique-inria

[15] http://www.scilab.org/fr/

[16] Benoit, C., Péron, S., and Landier, S., Cassiopee : a CFD pre- and post-processing tool, Aerospace Science and Technology, Vol. 45, pp. 275-283, 2015.

[17] http://www.openforam.com

[18] Palacios, F., Colonno, M. R., Aranake, A. C., Campos, A., Copeland, S. R., Economon, T. D., Lonkar, A. K., Lakaczyk, T. W., Taylor, T. W. R., and Alonso, J. J., Stanford University unstractured (SU^2): An open source integrated computational environment for multi-physics simulation and design, AIAA Paper 2013-0287, 51st AIAA Aerospace Meeting, Grapevine, Texas, 7-10 Jan. 2013.

[19] Paterson, E. G., Python scripting for gluing CFD applications : A case study demonstrating automation of grid generation, parameter variation,, flow simulation, analysis and plotting, Technical Report TR 09-001, The Pennsylvania State University, State College, 13 Jan. 2009 ;
[20] http://scikit-learn.org/stable/
[21] Schlichting, H., Boundary layer theory, 7th Ed., Mc Graw – hill, New-York, 1979.
[22] Weyburne, D., A mathematical description of the fluidboundary layer, Applied Mathematics and Computation, Vol. 175, pp. 1675-1684, 2006.
[23] Weyburne, D., New thickness and shape parameters for the boundary layer velocity profile, Experimental Thermal and Fluid Science, Vol. 54, pp. 22-28, 2014.
[24] Steelant, J., Private Communication, Excerpt from 'Roger Michel, Cours ENSAE', 26 Oct. 2017.